Article:
Zhao, Y., Moore, O.W., Xiao, K.-Q. et al. (4 more authors) (2023) Behavior and Fate of Chromium and Carbon during Fe(II)-Induced Transformation of Ferrihydrite Organominerals. Environmental Science & Technology, 57 (45). pp. 17501-17510. ISSN 0013-936X

https://doi.org/10.1021/acs.est.3c05487

Behavior and fate of chromium and carbon during Fe(II)-induced transformation of ferrihydrite organominerals

Yao Zhao, Oliver W. Moore, Ke-Qing Xiao*, Alba Otero-Fariña, Steven A. Banwart, Feng-Chang Wu*; Caroline L. Peacock

ABSTRACT

The mobility of chromium (Cr) is controlled by minerals, especially iron (oxyhydr)oxides. The influence of organic carbon (OC) on the mobility and fate of Cr(VI) during Fe(II)-induced transformation of iron (oxyhydr)oxide however, is still unclear. We investigate how low-weight carboxyl-rich OC influences the transformation of ferrihydrite (Fh) and controls the mobility of Cr(VI/III) in reducing environments, and how Cr influences the formation of secondary Fe minerals and the stabilization of OC. With respect to the transformation of Fe minerals, the presence of low-weight carboxyl-rich OC retards the growth of goethite crystals and stabilizes lepidocrocite for a longer time. With respect to the mobility of Cr, low-weight carboxyl-rich OC suppress the $Cr(III)_{non\text{-}extractable}$ associated with Fe minerals, and this suppression is enhanced with increasing carboxyl-richness of OC and decreasing pH. The presence of Cr(III) mitigates the decrease in total C associated with Fe minerals, and increase the $C_{non\text{-}extractable}$ especially for Fh organominerals made with carboxyl-rich OC. Our study sheds new light on the mobility and fate of Cr in reducing environments and suggests there is a potential synergy between Cr(VI) remediation and OC stabilization.

Keywords: chromium; Fe minerals; ferrihydrite; organic carbon; Fe(II); mobility

Synopsis

This study emphasizes the importance of interactions among Fe minerals, OC and heavy metals, which influence the properties of Fe minerals and control the mobility of OC and heavy metals in natural environments.

INTRODUCTION

Chromium is one of the most abundant elements in Earth's crust.[1,2,3] Depending on concentration

and valency, Cr is also one of the most common metal contaminants. Chromium (III) and (VI) are the two most common oxidation states, with Cr(III) predominating under reducing conditions, and Cr(VI) predominating under oxidizing conditions.[4] Cr(III) has a low solubility under natural conditions and readily precipitates as amorphous Cr(III) (hydr)oxide, limiting its mobility. The Cr(VI) oxyanion is highly soluble however, bioavailable and toxic, presenting a mobile biohazard in aquatic and soil ecosystems.[5-7] Despite this, the interactions between Cr and environmental constituents are still poorly understood, which limits our ability to predict its mobility and fate within environmental systems.

Ferrihydrite (Fh) is a common Fe (oxyhydr)oxide mineral in sediments with near ubiquitous occurrence.[8,9] Fh has large adsorption capacity,[10-12] making it the most efficient adsorbent for Cr and organic carbon (OC) in sediments.[13] On a global scale, more than 20% of organic carbon in sediments is directly associated with reactive iron phases.[13] Whereas, Fh is metastable and can be transformed to secondary Fe minerals via dissolution and re-crystallisation processes[14,15] and/or oriented aggregation process.[16] The transformation process of Fe minerals is significantly catalysed by Fe(II) under anoxic conditions, which controls the re-distribution of adsorbents like Cr and OC.

The transformation of Fh catalysed by Fe(II) may significantly impact the mobility and fate of Cr. [17,18] Under reducing conditions, highly mobile and toxic Cr(VI) readily oxidises Fe(II) to Fe(III) and itself is reduced to the low-mobility and toxic Cr(III) state.[19] This Cr(III) can be adsorbed by Fe (oxyhydr)oxides [20,21] and/or coprecipitated with Fe (oxyhydr)oxides, especially Fh and goethite (Gt).[22-30] Additionally, some Cr(VI) is found to be incorporated into Cr(III)-Fe(III) co-precipitates and exists under reducing conditions. [17,18] To date, few studies examine the role of OC in Cr migration during Fe(II)-catalyzed transformation of Fh organominerals, and find that humic acids immobilize more Cr by reducing Cr(VI) to Cr(III).[18] During transformation of Fh-Cr(III) coprecipitate, the presence of OC derived from rice straw can inhibit the transformation of Fh to Gt and thus decrease Cr(III) incorporation into Gt. In the system of Fh organominerals, Cr(III) preferentially associates with the Fh fraction, as observed by extended X-ray absorption fine structure spectroscopy,[21,31] whereas the OC may indirectly impact Cr(III) incorporation into Fe minerals through influencing mineral transformation products and crystal growth during Fe(II)-induced transformation of Fh.[32-37]

The stabilization of OC is also affected by the Fe(II)-induced transformation of Fh organominerals. [37,38] The reductive dissolution of Fh releases OC, making it more bioavailable for microbes, enhancing degradation of OC in sediments or soils.[38-41] The transformation of Fh however, may decrease the bioavailability of OC via occlusion within mineral structure defects or nano-pore spaces of Lp and Mg,[34,42] strengthening OC fixation in solids. One of the most important types of OC for Fe mineral-OC associations are carboxyl-rich OC. Carboxyl functional groups are prevalent in natural OC[43] and are highly reactive towards different metal ions, mineral surfaces and other adsorbents like microplastics.[44,45] Our recent NEXAFS spectroscopy and surface complexation modelling show that as the number of carboxyl functional groups present in simple OC increases, the number of carboxylate-Fe bonds formed between carboxyl functional groups and the Fe particles increases, and thus the binding strength and stability of the OC associated with Fh also increase.[46,47] At present, studies about OC stabilization during Fh transformation mainly involve the high-weight OC like fulvic acids, polygalacturonic acid, soil organic matter, and dissolved organic matter from litter sample,[37,42,48-50]. When OC gradually changes from low-weight OC to high-weight OC with increasing carboxyl-richness and binding strength, the mechanisms of OC stabilization are still ambiguous. Therefore, it is important to investigate how OC with different carboxyl-richness influence the transformation pathway of Fh and then influence the OC stabilization in reductive environment.

The stabilization of OC may also be influenced by other adsorbates on Fh. Anions like phosphate and arsenate can compete with OC for adsorption sites, increasing the desorption of OC,[51] whilst polycations like Ca(II) and Mg(II) may increase the OC sequestration by cation-bridging effects, forming iron (oxyhydr)oxide-cation-OC ternary complexes.[44,52,53] Prior study reports that during reductive transformation of Fh, the formation of nanopores in products facilitates the sequestration of OC, but high Cr(III) loading could impede the transformation of Fh and formation of nanopores, unfavoring OC stabilization.[50] The mechanisms behind OC stabilization in the presence of Cr(III) are still ambiguous for different pH conditions and for OC with different carboxyl richness and binding strength.

To address these knowledge gaps, we focus on the effect of carboxyl-rich OC and use simple mono-, di- and tri- carboxylic acids as model carboxyl-rich compounds, possessing increasing carboxyl-richness and thus increasing binding strengths to Fh. This study aims to (1) determine how different low-weight carboxyl-rich organic molecules and Cr(III) influence the mineralogical

transformation of Fh; (2) investigate how OC carboxyl-richness impacts the mobility of Cr during the Fe(II)-induced transformation of Fh organominerals; and (3) investigate how Cr(III) influences the properties of secondary Fe minerals and the stabilization of OC during the transformation process.

MATERIALS AND METHODS

Synthetic Fh and Fh organominerals. Pure ferrihydrite (Fh) was prepared by rapid hydrolysis of 0.1 M $Fe(NO_3)_3 \cdot 9H_2O$ (aq) with 1 M KOH to maintain a final pH of 7.[54] After several washes with DI water over a week, Fh was stored as a slurry at 4 ^oC to maintain mineralogical integrity.[54] Three Fh-OC organomineral composites with different wt%C were prepared with three simple carboxylic acids, denoted as acid, where acid refers to the first three letters of the acid IUPAC name. The acids used were pentanoic acid (Pen), hexanedioic acid (Hex) and butane 1, 2, 4 tricarboxylic acid (But), which have one, two and three carboxyl functional groups, respectively. These acids are prevalent in sediment and soil porewaters and here they also represent as model organic compounds for understanding the role of carboxyl richness in the mobility of Cr.[46,47] The 0.1 M $Fe(NO_3)_3 \cdot 9H_2O$ (aq) solutions were mixed with different organic acid solutions prior to hydrolysis at pH 7 as above for the pure Fh. An aliquot of each composite was then freeze-dried for C concentration analysis with LECO SC-144DR Dual Range Sulphur and Carbon Analyzer (LECO). As a result, three organominerals were obtained: Fh-pentanoic acid with 8.7 wt%C with molar ratio OC/Fe=0.816 (Fh_Pen_8.7wt%C), Fh-hexanedioic acid with 8.4 wt%C with molar ratio OC:Fe=0.810 (Fh_Hex_8.4wt%C) and Fh-butane 1, 2, 4 tricarboxylic acid with 8.1wt%C and 10.1 wt%C with OC:Fe molar ratios at 0.793 and 1.05 respectively (Fh_But_8.1wt%C and Fh_But_10.1wt%C). Our Fh organominerals have OC:Fe molar ratio around 1, which are lower than the average C:Fe ratios at 4 in sediments.[13]

Procedures of Fe(II)-induced Experiments. The Fe(II)-induced transformation experiments were conducted with batch experiments and the procedure is detailed in Section S1. All the solutions were purged with high purity N_2 for 0.5 h before being transferred into the glove box (95% N_2 and 5% H_2), and then equilibrated for 24 h to remove trace O_2. The experiments were conducted in the room without direct sunlight, and the control experiment in the dark environment show that the gentle natural light has negligible influences on Cr speciation in our experiment. An aliquot of the non-freeze-dried pure Fh and Fh organomineral slurries were added to 0.01 M

$NaNO_3$ background electrolyte to give a total volume of 50 mL with a solid solution ration of 2 g L^{-1} in the presence or absence of 20 ppm Cr(VI) at pH 5.75 or pH 7.00. Fe(II) were added into different systems when the reaction equilibrium between Cr(VI) and Fh organominerals were reached over 48 hours. The addition of Fe(II) to the systems was controlled to avoid the formation of magnetite which is favored at Fe(II)/Fh > 1 mmol Fe(II) / g Fh.[55-57] For systems with 0.385 mM (20 ppm) Cr(VI), 1.88 mM Fe(II) were added into suspensions. After the reaction between Fe(II) and Cr(VI), 0.725 mM Fe(II) are left in systems (0.363 mmol Fe(II)/g Fh). For systems without Cr(VI), Fe(II) was also controlled at 0.725 mM to observe how Cr influences transformation of Fh. The concentrations of aqueous Fe(II) and Fe(II) sorbed on particle surfaces were measured (methods in Section S2 and results in Section S5). The suspensions were collected at time intervals of 0.5 h, 1 d, 2 d, 4 d, 6 d, 8 d, 12 d, 18 d and 90 d to investigate mineralogical transformation, Cr distribution and OC stabilization.

Chromium speciation and distribution. The potential mobility of Cr(III) was evaluated by treatment with desorbing solutions (see comparison between different extraction methods, supporting information Section S4). As thus, the distribution of Cr was operationally defined as aqueous, extractable and non-extractable Cr. The aqueous Cr(VI) was measured with a spectrometric method that uses 1,5-diphenylcarbazide[58,59] and total Cr(VI and III) were measured by inductively coupled plasma mass spectrometry (ICP-MS). Cr(VI and III) in the extractable pool were tracked with the desorbing solution (200 ppm $KMnO_4$ and 0.1 M NaOH mixture solution, 24 h), which was operationally defined as $Cr_{KMnO4\text{-}NaOH\text{-}extractable}$. The non-extractable Cr ($Cr_{non\text{-}extractable}$) was calculated based on the mass balance. Dissolution kinetics of the final products were also studied using 3 M HCl solution at 40 ℃ over 74 h (Section S8).

OC stabilization. Two 15 mL aliquots of suspension were filtered with 0.22 μm cellulose nitrate filters using a vacuum filtration system. The mineral particles were rinsed using 15 mL DI water, collected and freeze-dried for total solid C measurement using LECO. The other mineral particle subsample was re-suspended in 15 mL 0.1 M NaOH and shaken for 24 h to extract OC from the solid.[60] Then the mineral particles were filtered with 0.22 μm PES filters, washed and freeze-dried for C concentration measurement, which was operationally defined as non-extractable OC ($C_{non\text{-}extractable}$).

Solid-Phase Analysis. FTIR spectra of the solid mineral phase were collected using Attenuated Total Reflectance Fourier Transform Infrared Spectroscopy (ATR-FTIR) (Agilent

4500a FTIR with an ATR) to observe changes in iron mineralogy and the respective proportions of each mineral phase[61,62] (Section S2). FTIR spectra were obtained by accumulating 64 scans over an energy range of 650 to 4000 cm^{-1} with a spectral resolution of 4 cm^{-1}. The relative proportions of Lp and Gt were calculated using the measured absorbances at 1020 cm^{-1} and 890 cm^{-1}, respectively.[62,63] Information about crystallinity of iron minerals was obtained by tracking changes in OH stretching vibrations[9] from 2600 cm^{-1} to 3800 cm^{-1} which includes non-stoichiometric hydroxyls and stoichiometric (or bulk) OH groups[64] with a shoulder at lower frequencies[65] (Section S3). The secondary iron minerals were also identified by Raman spectra obtained with Renishaw in-Via Raman Spectrometer at 785 nm laser and by X-ray diffraction spectra (XRD) obtained with a Bruker D8 ADVANCE diffractometer with Cu-Kα radiation (γ=0.514 nm).

A transmission electron microscope (TEM) Japan-JEOL-JESM 2100F equipped with energy dispersive X-ray spectroscopy (EDS) was applied to analyze the morphology and elemental distribution of selected samples. The samples were sonicated in acetone for 20 min at 25 ℃ and subsequently dropped onto a Si_3N_3 membrane to exclude interference from the C background.[42] EDS line profiles of elements were used to analyze the Fe, Cr and C distributions. The oxidation states of the Cr present on the surface of secondary Fe minerals were determined via X-ray photoelectron spectroscopy (XPS) (Thermlfisher ESCALAB250Xi). To avoid the oxidation of Cr(III) by Fenton reaction induced by Fe(II) and O_2, the secondary Fe minerals were washed with MilliQ-water twice in the anoxic box, and then freeze-dried for XPS analysis.

RESULTS AND DISCUSSION

Mineralogical transformation of iron minerals. The transformation of Fh to secondary Fe minerals were tracked with FTIR, where bands at 1020 and 743 cm^{-1} are characteristic bands of Lp whilst bands at 895 and 793 cm^{-1} are recognized as Gt. The proportions of Lp or Gt were calculated and shown in Figure 1. In all systems the proportion of Gt increases with reaction time, whilst the proportion of Lp generally peaks and then decreases (Fig. 1), suggesting the presence of transformation pathway from Lp to Gt. The selected secondary iron minerals are also characterized by XRD and Raman. In XRD patterns, goethite (peaks at 17.8°, 21.26°, 26.4°, 33.3°, 34.7°, 36.7° etc.) is the only Fe mineral identified in pure Fh systems, but both Lp (peaks at 14.17°, 27.14° and 36.37° etc.) and Gt are identified in Fh_But systems after 12-days reaction (Fig. S10). Similarly, in Raman spectra only peaks for Gt (243, 297, 384 and 477 cm^{-1}) are observed in pure

Fh, Fh_Pen and Fh_Hex2/5 systems, whilst peaks for both Gt and Lp (250 and 284 cm^{-1}) are observed in Fh_But systems (Fig. S11) even after 90-days reaction. Therefore, Gt and Lp are the only secondary iron minerals in our experiment.

In presence of OC, the transformation rate of Fh decreases with the increasing carboxyl-richness of the OC and follows the order Pen1/7 <pure Fh ~ Hex < But at similar OC/Fe ratios (Fig. 1). Compared with Pen and Hex, the tri-carboxylic But acid more effectively inhibits the transformation of Fh to secondary Fe minerals at pH 5.75. Nonetheless, $Fe(II)_{adsorbed}$ in Fh_But system is twice more than that for other systems (0.23 mM $Fe(II)_{adsorbed}$ for Fh_But vs. ~0.1 mM $Fe(II)_{adsorbed}$ for others, at pH 5.75) (Fig. S5). As such, But acid probably inhibits the transformation process of Fh by blocking mineral surface sites[66,67] to inhibit the dissolution-recrystallization processes, and/or by chelating with Fe(II)[37] to inhibit the reaction between Fe(II) and Fe(III) with the Fe mineral structure. In addition, tri-carboxylic But acid may also form a negatively charge coating on mineral particles that then repel one another,[68] or acting as bridge between mineral particles[68,69] and thus hindering aggregation and growth of Gt.[70] Specifically, the tri-carboxylic But acid can provide more carboxyl functional groups to enhance the inhibitive influences on transformation of Fe minerals compared to carboxyl-poor OC. It is also observed that tri-carboxylic But acid in Fh_But_10.1wt%C experiment effectively stabilizes Lp for a longer time compared with other systems at pH 5.75 and 7.00 (Fig. 1, S8, S10 and S11), probably via mechanisms mentioned above.[37] Whereas, the influences of mono-carboxylic Pen acid and di-carboxylic Hex acid on the stabilization of Lp are not discernable, which needs further investigation. Compared with pure Fh systems, the crystal size of Gt formed in Fh_But_8.1wt%C systems are smaller after 12-days reaction based on XRD patterns (Fig.S10). The morphology images by TEM also show that Gt formed from Fh_But_10.1wt%C has smaller crystal size (Fig. S9a vs. S9e), a loose structure (Fig. S9b vs. S9f) and larger lattice spacing (Fig. S9d vs. S9h) than that formed from pure Fh after 90-days reaction. During the acid-digestion of final transformation products, Fe release are much faster in Fh_But systems than in pure Fh systems at pH 7, suggesting secondary Fe minerals formed in the presence of OC has higher chemical reactivity (Fig. S13). Therefore, it seems that OC with higher binding strength tends to more effectively inhibit the transformation of Fh and the crystal growth of Gt, but facilitate the stabilization of Lp for longer time. Previous studies documented that high-weight OC (e.g. OC extracted from fresh litter samples,[37] river DOM[71] and fulvic acid[34] which have much higher carboxyl richness) could even

completely inhibit the transformation of Fh, or lead to sole products of Lp at the comparable experiment conditions to ours. As such, it is speculated that when OC gradually changes from low-weight OC to high-weight OC with increasing carboxyl-richness and binding strength, the suppression on the transformation process will be increasingly enhanced.

The presence of Cr(III) appear to inhibit the transformation from Lp to Gt in the pure Fh system, Fh_Pen_8.7wt%C and Fh_But_10.1wt%C experiments at pH 7.00 (Fig. 1). For Fh_But_8.1wt%C systems at pH 7.0, TEM images also show that Fe mineral particles appears to have loose structure in the presence of Cr (Fig S7), suggesting lower crystallinity than that formed in the absence of Cr. The possible reason is that Cr(III) adsorbed onto Lp surface hinders the dissolution and recrystallization process of Lp to form Gt,[72] which is supported by previous studies that the presence of adsorbates like As(V) favor the formation of Lp.[34]

The rates for the formation of Gt and Lp are generally higher at pH 7.00 than at pH 5.75 (Fig. 1). In all systems, $Fe(II)_{adsorbed}$ ranged from 0.4 mM to 0.6 mM at pH 7.00, which are much higher than $Fe(II)_{adsorbed}$ (~0.1 mM) at pH 5.75 (Fig. S5). The lower amount of Fe(II) adsorbed on the mineral surface at lower pH may result in less Fe atom exchange between aqueous Fe(II) and Fe(III) within the mineral structure[67] and slower dissolution and recrystallisation processes.

Redistribution of Cr. As shown in Fig. 2, no aqueous Cr(VI) or Cr(III) are detected throughout the whole transformation process, and therefore all Cr is associated with the solid minerals. Most Cr(VI) is reduced to Cr(III) by Fe(II) within 0.5 h, because Cr(VI) and Fe(II) are very strong oxidants and reductants, respectively. The observed increase in the $Cr_{non\text{-}extractable}$ pool with time originates from the $Cr(III)_{KMnO4\text{-}NaOH\text{-}extractable}$ pool.

Regarding the transition of Cr from extractable pool to non-extractable pool, several mechanisms are supposed. Initially Cr is adsorbed onto Fh surface, and then some Cr are incorporated into Gt particles with reaction processing, which are supported by the TEM observation and acid-digestion results. For signal crystal (Fig. 3a), the peaks of Cr signal appear at the edge of Fe signal suggesting the existence of Cr adsorbed/precipitated on mineral surface, whilst Cr and Fe signal reach peaks at the same position, suggesting the incorporation of Cr into Gt minerals via substitution[25,28,73] or occlusion.[74] For the aggregation growth of Gt nano-particles (Fig. 3b), the Fe signal reach the valley but Cr signal reach the peak, the position of which are corresponding to the spaces between Gt nano-particles. It indicates that analogue to C and Pb,[74] Cr in our systems might also be occluded during the aggregation growth of Gt nano-particles. Our

247 results of acid treatment show that 11% ~ 20% of total Cr were released with minor Fe dissolved
248 within 5 mins (Fig. S13), suggesting the presence of Cr adsorbed or precipitated on Fe mineral
249 surface in both pure Fh and Fh_But organomineral systems.[75] Then Cr were released gradually
250 with Fe release, yielding a convex relative curve same with prior study.[76] This indicates a non-
251 uniform distribution of Cr inside Fe minerals,[75] with more Cr-enrichment in outer layers than in
252 center layers.[29] Therefore, both TEM observation and acid-digestion results confirm the presence
253 of Cr adsorbed/precipitated on mineral surface, and Cr incorporation into Fe minerals during the
254 transformation process.
255 In addition, the cloud-like Fe minerals are observed in Fh systems at pH 7 after reacting for
256 12 days (Fig. 3c). Together with EDS line profile that Cr shows a positive relationship with Fe
257 signal, the remain Fh-like phase is regarded as Fe-Cr coprecipitate. Previous work demonstrate
258 that $Cr_xFe_{1-x}(OH)_3$ could occur as a solid solution, where the reactivity of $Fe(OH)_3$ decreased in
259 the presence of Cr.[77] It is also reported that Cr(III) becomes more concentrated in the residual Fh
260 compared to the initial Fh,[76] where the Cr(III) may co-precipitated with Fh. As such, Fe-Cr
261 coprecipitates appear to be more stable than pure Fh, and thus might stabilize for longer time. For
262 the Cr 2p XPS spectra, the peaks at 579.6 and 589.0 eV are assigned as Cr(VI) which account for
263 18.9% of total Cr on mineral surface, whilst the peaks at 577.3 and 586.8 eV are assigned as Cr(III)
264 which are dominant species on mineral surface. Considering the strong reducibility of Fe(II), these
265 Cr(VI) in systems may be incorporated into Fe-Cr coprecipitates and thus escape the attack of
266 Fe(II).[17]
267 Regarding the influences of OC, the final proportion of $Cr_{non\text{-}extractable}$ decreases with
268 increasing carboxyl-richness of the sequestered OC and generally follows the order pure Fh ~
269 Fh_Pen_8.7wt%C > Fh_Hex_8.4wt%C > Fh_But_10.1wt%C at pH 5.75 and 7.00 after 90 days
270 reaction (Fig. 2). One possible reason for the decrease in the final proportion of $Cr_{non\text{-}extractable}$ is
271 that OC inhibits the formation of Gt which could host Cr up to 10 % (mole ratio) inside Gt mineral
272 via many mechanisms.[9,78] In contrast, the incorporation of Cr(III) into Lp minerals in a large
273 amount has not been reported.[9] Our EDS line profiles show that Cr signal at the edge of Lp are
274 much higher than that in the bulk of Lp minerals, which is a typical character of Cr
275 adsorbed/precipitated on the Lp surface (Fig. 4a). The carboxyl-rich OC (like But in our
276 experiments) favors the formation of Lp and stabilizes Lp at a high proportion for a longer time,
277 which could lessen the amount of $Cr_{non\text{-}extractable}$ associated with Fe minerals. Alternatively, the

presence of OC also inhibits the aggregation growth of Gt nano-particles leading to smaller crystal size of Gt particles (Fig. S9 and S10), and then suppresses the encapsulation of Cr inside the spaces between Gt nano-particles. Prior study reported that humic acid completely inhibit the transformation of Fh to Gt, and thus inhibit the incorporation of Cr(III) into Gt formed.[21] As discussed above, when OC gradually changes from low-weight OC to high-weight OC with increasing carboxyl-richness and binding strength, the transformation of Fh is expected to be further inhibited, where the growth and aggregation of Gt nano-particles is suppressed but the formation of Lp is favored. In this scenario, the presence of higher-weight OC could result in lower amount of Cr(III) incorporation into Gt and more Cr(III) will be retained in the $KMnO_4$-NaOH extractable pool.

Table 1. The elevation of $C_{total\text{-}solid}$ by Cr(III) after 18-days Fe(II)-induced transformation of Fh organominerals at pH 5.75

	$C_{total\text{-}solid}$_no Cr (wt%C)	$C_{total\text{-}solid}$_Cr (wt%C)	$C_{total\text{-}solid}$ elevated by Cr (wt%C)	Percentage of $C_{total\text{-}solid}$ elevated by Cr
Fh_Pen_8.7wt%C	0.52±0.025	0.65±0.016	0.13	25%
Fh_Hex_8.4wt%C	2.68±0.084	2.96±0.059	0.28	21%
Fh_But_10.1wt%C	4.80±0.046	5.82±0.023	1.02	21%

Stabilization of OC. The $C_{total\text{-}solid}$ associated with the minerals generally decreases with reaction time, which is consistent with previous studies[74,79] and the decrease is enhanced at pH 7.00 (Fig. 5). Our EDS line profile indicates that OC is mainly located on the Gt surface (Fig. 4b). Thus, the decrease in $C_{total\text{-}solid}$ is attributed to the increase in crystallinity and the decrease in specific surface area (SSA) of Fe minerals.[80-85] As shown in Fig. 1, the transformation of Fh to Gt/Lp is faster at pH 7.00, which leads to a sharp decrease in SSA of Fh minerals and thus a sharp decrease in $C_{total\text{-}solid}$. Additionally, the adsorption of OC decreases with increasing pH conditions,[86] which also enhances the decrease in $C_{total\text{-}solid}$ at pH 7.00.

The $C_{total\text{-}solid}$ over the reaction appears to increase with the carboxyl-richness of the OC and follows the order Fh_Pen_8.7 wt%C < Fh_Hex_8.4 wt%C < Fh_But_10.1 wt%C. This is probably because the stabilization of OC is also controlled by its adsorption affinity to iron minerals, where OC with higher carboxyl-richness has higher affinity to Fe minerals[46,47] and tends to persist for a

304 longer time in natural environments.[46,87] Also OC with higher carboxyl-richness tends to
305 effectively inhibit the transformation of Fh or Lp (Fig. 1), which also stabilizes more OC associated
306 with the solids.[86] Prior studies reported that ~15% of FA were released from minerals[34] and non-
307 discernable DOM were released[37] during the Fe(II)-induced transformation of Fh-OC
308 coprecipitates at pH 7, which were much lower than ours with 70% and 45% of OC released for
309 Fh_Hex and Fh_But systems, respectively. Therefore, it implies that the stability of OC associated
310 with minerals will gradually increase, when OC gradually changes from low-weight OC to high-
311 weight OC with increasing carboxyl-richness and binding strength.
312 The presence of Cr(III) aids OC stabilization with the solid phase at pH 5.75 after 18-days
313 reaction (Fig. 5), where typically But associated with minerals are elevated by 1 wt%C whilst
314 percentage of $C_{total\text{-}solid}$ elevated by Cr(III) for all organomineral systems are around 20% (Table
315 1). A potential reason is that analogue to As(V),[34] Cr(III) inhibits the transformation process of Fh
316 or stabilize Lp for longer time (Fig. 1), allowing more OC to be adsorbed. Based on our FTIR data,
317 the presence of Cr(III) leads to more structural defects and lower crystallinity of Fe minerals, and
318 results in higher surface OH reactivity (Section 3 and 6), or a combination of these, which results
319 in more OC stabilized with Fe minerals. Whereas, the elevation of $C_{total-solid}$ by Cr(III) is weakened
320 with reaction time at pH 7.00 (Fig. 5), which are attributed to the increase in the crystallinity of
321 Fe minerals with reaction time.
322 The operationally defined $C_{non\text{-}extractable}$ indicates that OC may be very strongly bound onto the
323 mineral surface,[46,88] or incorporated into the interior of aggregates.[74,89,90] The different changes in
324 $C_{non\text{-}extractable}$ for OC with different binding strength are observed in our previous work,[47] where
325 $C_{non\text{-}extractable}$ for OC (Pen and Hex) with lower binding strength appear to decrease whilst $C_{non\text{-}}$
326 $_{extractable}$ for OC (But) with higher binding strength generally show a stable trend with aging process
327 under oxic conditions. By contrast, $C_{non\text{-}extractable}$ for OC (But) with higher binding strength shows
328 an increasing trend during the Fe(II)-induced transformation of Fh_But organominerals (Fig. 6).
329 Our EDS line profiles for Lp show that C signal peaks at the position of the structure defects or
330 pore spaces of Lp (Fig. 4a), suggesting the occlusion of OC inside. As the strongly-bound OC (like
331 But in our systems) can stabilize Lp for longer time (Fig.1), the incorporation of OC into Lp
332 mineral[34, 42] could be facilitated. In addition, our EDS line profiles show that C signal is positively
333 related with Fe signal (Fig. 4c), which suggests the incorporation of C into the bulk Fe minerals.

As such, it is speculated that OC may be occluded inside mineral aggregate, leading to the increasing $C_{non\text{-}extractable}$.

The presence of Cr seems to increase $C_{non\text{-}extractable}$ for Fh_Hex_8.4wt%C and Fh_But_10.1wt%C (Fig. 6), suggesting that Cr(III) aids OC sequestration inside Fe minerals. One possible mechanism is that the presence of Cr(III) facilitate and stabilize Lp for longer time, especially in Fh_But_10.1wt%C systems (Fig. 1d). The structure defects of Lp (Fig. 4) contribute to OC occlusion inside minerals.[34] Another possible mechanism may be that Cr(III) polymers/precipitates on mineral surface act as a good substrate for Fe(III) to precipitate around, or for the already formed iron mineral particles to aggregate around, which weaken the influence of OC on the aggregation of Fe mineral particles due to electrostatic repulsion.[68] As thus Cr(III) facilitate the aggregation of Fe mineral particles and occlude some OC in pore spaces.

The increase in $C_{non\text{-}extractable}$ elevated by Cr(III) appears to be weakened with decreasing binding strength of OC. There is no difference in $C_{non\text{-}extractable}$ for Fh_Pen_8.7wt%C (Fig. 6), probably because OC with lower binding strength is readily desorbed from the mineral particles during the aggregation process. By contrast, OC with higher binding strength is more stable against desorption and can be sequestered in mineral aggregates.

ENVIRONMENTAL SIGNIFICANCE

The results of this study demonstrate that the carboxyl-richness of low-weight OC plays an important role in controlling the mobility of Cr in Fe minerals and conversely Cr(III) influences the stabilization of low-weight OC associated with Fe minerals. As such this study sheds new light on the behavior of Cr in natural sedimentary environments with changing redox conditions. This study predicts that under anoxic conditions, Cr(III) reduced from Cr(VI) will preferentially exist in the solid phase as adsorbates or precipitates, but that this Cr(III) will still have a high potential for re-mobilization or oxidation to Cr(VI). As such the capture of Cr(III) inside Fe minerals is likely a relatively stable and reliable pathway for the sequestration of Cr in sediments or soils, which is influenced by carboxyl-rich OC and pH. This work reveals that low-weight carboxyl-rich OC in sediments or soils will suppress $Cr(III)_{non\text{-}extractable}$ associated with Fe minerals, and this suppression will be enhanced with increasing carboxyl-richness of OC and decreasing pH conditions. It is expected that when OC gradually changes from low-weight OC to high-weight OC with increasing carboxyl-richness and binding strength, the transformation of Fh is expected

to be further inhibited, with the growth and aggregation of Gt nano-particles suppressed, which result in more Cr retained in $KMnO_4$-NaOH extractable pool. A lower pH of sediments or soils will likely increase the adsorption of carboxyl-rich OC onto Fe minerals and thus enhance the inhibitory influences of OC on Cr(III) captured inside Fe minerals. Conversely, Cr(III) reduced from Cr(VI) may aid more OC stabilization with solid minerals. In addition, Cr(III) also appears to stabilize Lp for longer time especially in the presence of carboxyl-rich OC (like tri-carboxylic acid But), and thus facilitate the accumulation of $C_{non\text{-}desorbable}$ associated with Lp. As such the best scenario for Cr remediation and the preservation of OC might be achieved that the suppression of Cr(III) captured inside Fe minerals is less significant, whilst Cr(III) aids OC stabilization with Fe minerals.

ASSOCIATED CONTENT

Supporting information

Additional experimental details, methods, Fe(II) variations, FTIR analysis and dissolution kinetics. Tables showing the different extraction methods. Figures showing structure of carboxylic acids, FTIR spectra, Raman spectra, XRD spectra, XPS spectra, variation in OH-stretching bands and TEM images as well as acid-digestion results.

AUTHOR INFORMATION

Corresponding authors

Feng-Chang Wu - *State Key Laboratory of Environmental Criteria and Risk Assessment, Chinese Research Academy of Environmental Sciences, Beijing 100012, China;* E-mail: wufengchang@vip.skleg.cn

Ke-Qing Xiao - *State Key Lab of Urban and Regional Ecology, Research Center for Eco-Environmental Sciences, Chinese Academy of Sciences, Beijing, China;* E-mail: kqxiao@rcees.ac.cn

Authors

Yao Zhao - *State Key Laboratory of Environmental Criteria and Risk Assessment, Chinese Research Academy of Environmental Sciences, Beijing 100012, China; School of Earth & Environment, University of Leeds, Leeds, LS2 9JT, UK;*

Oliver W. Moore - *School of Earth & Environment, University of Leeds, Leeds, LS2 9JT, UK*

Alba Otero-Fariña - *School of Earth & Environment, University of Leeds, Leeds, LS2 9JT, UK*
Steven A. Banwart - *School of Earth & Environment, University of Leeds, Leeds, LS2 9JT, UK*
Caroline L. Peacock - *School of Earth & Environment, University of Leeds, Leeds, LS2 9JT, UK*

ACKNOWLEDGMENTS

We thank laboratory managers Andrew Hobson and Stephen Reid, and laboratory technician Fiona Keay and Yi-Jun Xiong (University of Leeds) for laboratory support. This research project has received funding from the National Natural Science Foundation of China (no. 42307316) and the European Research Council (ERC) under the European Union's Horizon 2020 research and innovation programme (Grant agreement No. 725613 MinOrg). A. O. F. and C. L. P. gratefully acknowledge NERC Highlight Topic Grant (NE/S004963/1 Locked Up). Y. Z. gratefully acknowledges support from the China Scholarship Council. C. L. P. gratefully acknowledges Royal Society Wolfson Research Merit Award (WRM/FT/170005). K-Q. X. is funded by the Hundred Talents Program of the Chinese Academy of Sciences.

Notes

The authors declare no competing financial interest.

REFERENCES

(1) Shahid, M.; Shamshad, S.; Rafiq, M.; Khalid, S.; Bibi, I.; Niazi, N. K.; Dumat, C.; Rashid, M. I., Chromium speciation, bioavailability, uptake, toxicity and detoxification in soil-plant system: A review. *Chemosphere* **2017,** *178*, 513-533.

(2) Jeejeebhoy, K. N.; Chu, R.; Marliss, E.; Greenberg, G. R.; Bruce-Robertson, A., Chromium deficiency, glucose intolerance, and neuropathy reversed by chromium supplementation, in a patient receiving long-term total parenteral nutrition. *Am. J. Clin. Nutr.***1977,** *30*, (4), 531-538.

(3) Schwarz; K. , M.; W., A glucose tolerance factor and its differentiation from factor. *Arch. Biochem. Biophys.* **1957,** *72*, (2), 515-518.

(4) Richard, F. C.; Bourg, A. C., Aqueous geochemistry of chromium: a review. *Water Res.* **1991,** *25*, (7), 807-816.

(5) Chandra, P.; Kulshreshtha, K., Chromium accumulation and toxicity in aquatic vascular plants. *Bot. Rev.* **2004,** *70*, (3), 313-327.

(6) Shanker, A. K.; Cervantes, C.; Loza-Tavera, H.; Avudainayagam, S., Chromium toxicity in plants. *Environ. Int.* **2005,** *31*, (5), 739-753.

(7) Costa, M., Toxicity and Carcinogenicity of Cr(VI) in Animal Models and Humans. *Crit. Rev. Toxicol.* **1997,** *27*, (5), 431-442.

(8) Lu, Y.; Hu, S.; Liang, Z.; Zhu, M.; Wang, Z.; Wang, X.; Liang, Y.; Dang, Z.; Shi, Z., Incorporation of Pb(ii) into hematite during ferrihydrite transformation. Environ. Sci.: Nano **2020,** *7*, (3), 829-841.

(9) Cornell, R. M.; Schwertmann, U., *The iron oxides: structure, properties, reactions, occurrences and uses*. Weinheim, VCH.: 2003.

(10) Michel, F. M.; Ehm, L.; Liu, G.; Han, W. Q.; Antao, S. M.; Chupas, P. J.; Lee, P. L.; Knorr, K.; Eulert, H.; Kim, J.; Grey, C. P.; Celestian, A. J.; Gillow, J.; Schoonen, M. A. A.; Strongin, D. R.; Parise, J. B., Similarities in 2- and 6-Line Ferrihydrite Based on Pair Distribution Function Analysis of X-ray Total Scattering. *Chem. Mater.* **2007,** *19*, (6), 1489-1496.

(11) Hiemstra, T., Surface and mineral structure of ferrihydrite. *Geochim. Cosmochim. Acta* **2013,** *105*, 316-325.

(12) Larsen, O.; Postma, D., Kinetics of reductive bulk dissolution of lepidocrocite, ferrihydrite, and goethite. *Geochim. Cosmochim. Acta* **2001,** *65*, (9), 1367-1379.

(13) Lalonde, K.; Mucci, A.; Ouellet, A.; Gélinas, Y., Preservation of organic matter in sediments promoted by iron. *Nature* **2012,** *483*, 198.

(14) Tronc, E.; Belleville, P.; Jolivet, J. P.; Livage, J., Transformation of ferric hydroxide into spinel by iron(II) adsorption. *Langmuir* **1992,** *8*, (1), 313-319.

(15) Pedersen, H. D.; Postma, D.; Jakobsen, R.; Larsen, O., Fast transformation of iron oxyhydroxides by the catalytic action of aqueous Fe(II). *Geochim. Cosmochim. Acta* **2005,** *69*, (16), 3967-3977.

(16)Yan, W.; Liu, H.; Chen, R.; Xie, J.; Wei, Y., Dissolution and oriented aggregation: transformation from lepidorocite to goethite by the catalysis of aqueous Fe(ii). *RSC Adv.* **2015,** *5*, (129), 106396-106399.

(17) Hu, Y.; Xue, Q.; Tang, J.; Fan, X.; Chen, H., New insights on Cr(VI) retention by ferrihydrite in the presence of Fe(II). *Chemosphere* **2019,** *222*, 511-516.

(18) Yu, G.; Fu, F.; Ye, C.; Tang, B., Behaviors and fate of adsorbed Cr(VI) during Fe(II)-induced transformation of ferrihydrite-humic acid co-precipitates. J. Hazard. Mater.**2020,** *392*, 122272.

(19) Buerge, I. J.; Hug, S. J., Kinetics and pH Dependence of Chromium(VI) Reduction by Iron(II). *Environ. Sci. Technol.* **1997,** *31*, (5), 1426-1432.

(20) Richard, F. C.; Bourg, A. C. M., Aqueous geochemistry of chromium: A review. *Water Res.* **1991,** *25*, (7), 807-816.

(21) Xia, X.; Yang, J.; Yan, Y.; Wang, J.; Hu, Y.; Zeng, X., Molecular Sorption Mechanisms of Cr(III) to Organo-Ferrihydrite Coprecipitates Using Synchrotron-Based EXAFS and STXM Techniques. *Environ. Sci. Technol.* **2020,** *54*, (20), 12989-12997.

(22) Namgung, S.; Kwon, M. J.; Qafoku, N. P.; Lee, G., Cr(OH)3(s) Oxidation Induced by Surface Catalyzed Mn(II) Oxidation. *Environ. Sci. Technol.* **2014,** *48*, (18), 10760-10768.

(23) Trolard, F.; Bourrie, G.; Jeanroy, E.; Herbillon, A. J.; Martin, H., Trace metals in natural iron oxides from laterites: A study using selective kinetic extraction. *Geochim. Cosmochim. Acta* **1995,** *59*, (7), 1285-1297.

(24) Hua, J.; Chen, M.; Liu, C.; Li, F.; Long, J.; Gao, T.; Wu, F.; Lei, J.; Gu, M., Cr Release from Cr-Substituted Goethite during Aqueous Fe(II)-Induced Recrystallization. *Clay Miner.* **2018,** *8*, (9), 367.

(25) Charlet, L.; Manceau, A. A., X-ray absorption spectroscopic study of the sorption of Cr(III) at the oxide-water interface: II. Adsorption, coprecipitation, and surface precipitation on hydrous ferric oxide. *J. Colloid Interface Sci.* **1992,** *148*, (2), 443-458.

(26) Manceau, A.; Schlegel, M. L.; Musso, M.; Sole, V. A.; Gauthier, C.; Petit, P. E.; Trolard, F., Crystal chemistry of trace elements in natural and synthetic goethite. *Geochim. Cosmochim. Acta* **2000,** *64*, (21), 3643-3661.

(27) Maslar, J. E.; Hurst, W. S.; Bowers, W. J.; Hendricks, J. H.; Aquino, M. I.; Levin, I., In situ Raman spectroscopic investigation of chromium surfaces under hydrothermal conditions. *Appl. Surf. Sci.* **2001,** *180*, (1), 102-118.

(28) Tang, Y.; Michel, F. M.; Zhang, L.; Harrington, R.; Parise, J. B.; Reeder, R. J., Structural Properties of the Cr(III)−Fe(III) (Oxy)hydroxide Compositional Series: Insights for a Nanomaterial "Solid Solution". *Chem. Mater.* **2010,** *22*, (12), 3589-3598.

(29) Dai, C.; Zuo, X.; Cao, B.; Hu, Y., Homogeneous and Heterogeneous (Fex, Cr1-x)(OH)3 Precipitation: Implications for Cr Sequestration. *Environ. Sci. Technol.***2016,** *50*, (4), 1741-9.

(30) Choppala, G.; Burton, E. D., Chromium(III) substitution inhibits the Fe(II)-accelerated transformation of schwertmannite. *PLoS One* **2018,** *13*, (12).

(31) Xia, X.; Wang, J.; Hu, Y.; Liu, J.; Darma, A. I.; Jin, L.; Han, H.; He, C.; Yang, J., Molecular Insights into Roles of Dissolved Organic Matter in Cr(III) Immobilization by Coprecipitation with Fe(III) Probed by STXM-Ptychography and XANES Spectroscopy. *Environ. Sci. Technol.* **2022,** *56*, (4), 2432-2442.

(32) Zhou, Z.; Latta, D. E.; Noor, N.; Thompson, A.; Borch, T.; Scherer, M. M., Fe(II)-Catalyzed Transformation of Organic Matter-Ferrihydrite Coprecipitates: A Closer Look Using Fe Isotopes. *Environ. Sci. Technol.* **2018,** *52*, (19), 11142-11150.

(33) Karimian, N.; Burton, E. D.; Johnston, S. G., Antimony speciation and mobility during Fe(II)-induced transformation of humic acid-antimony(V)-iron(III) coprecipitates. *Environ. Pollut.* **2019,** *254*, 113112.

(34) Hu, S.; Liang, Y.; Liu, T.; Li, F.; Lu, Y.; Shi, Z., Kinetics of As(V) and carbon sequestration during Fe(II)-induced transformation of ferrihydrite-As(V)-fulvic acid coprecipitates. *Geochim. Cosmochim. Acta* **2020,** *272*, 160-176.

(35) Sheng, A.; Liu, J.; Li, X.; Qafoku, O.; Collins, R. N.; Jones, A. M.; Pearce, C. I.; Wang, C.; Ni, J.; Lu, A.; Rosso, K. M., Labile Fe(III) from sorbed Fe(II) oxidation is the key intermediate in Fe(II)-catalyzed ferrihydrite transformation. *Geochim. Cosmochim. Acta* **2020**, *272*, 105-120.

(36) Chen, C.; Sparks, D. L., Fe(II)-Induced Mineral Transformation of Ferrihydrite–Organic Matter Adsorption and Co-precipitation Complexes in the Absence and Presence of As(III). *ACS Earth Space Chem.* **2018,** *2*, (11), 1095-1101.

(37) Chen, C.; Kukkadapu, R.; Sparks, D. L., Influence of Coprecipitated Organic Matter on Fe2+(aq)-Catalyzed Transformation of Ferrihydrite: Implications for Carbon Dynamics. *Environ. Sci. Technol.* **2015,** *49*, (18), 10927-36.

(38) Chen, C.; Hall, S. J.; Coward, E.; Thompson, A., Iron-mediated organic matter decomposition in humid soils can counteract protection. *Nat. Commun.* **2020,** *11*, (1), 2255.

(39) Canfield, D. E., Jørgensen, B.B., Fossing, H., Glud, R., Gundersen, J., Ramsing, N.B., Thamdrup, B., Hansen, J.W., Nielsen, L.P. and Hall, P.O., Pathways of organic carbon oxidation in three continental margin sediments. . *Mar. Geol.* **1993,** *113*, 27-40.

(40) Adhikari, D.; Zhao, Q.; Das, K.; Mejia, J.; Huang, R.; Wang, X.; Poulson, S. R.; Tang, Y.; Roden, E. E.; Yang, Y., Dynamics of ferrihydrite-bound organic carbon during microbial Fe reduction. *Geochim. Cosmochim. Acta***2017,** *212*, 221-233.

(41) Han, L.; Sun, K.; Keiluweit, M.; Yang, Y.; Yang, Y.; Jin, J.; Sun, H.; Wu, F.; Xing, B., Mobilization of ferrihydrite-associated organic carbon during Fe reduction: Adsorption versus coprecipitation. *Chem. Geol.* **2019,** *503*, 61-68.

(42) Hu, S.; Zhen, L.; Liu, S.; Liu, C.; Shi, Z.; Li, F.; Liu, T., Synchronous sequestration of cadmium and fulvic acid by secondary minerals from Fe(II)-catalyzed ferrihydrite transformation. *Geochim. Cosmochim. Acta* **2022,** *334*, 83-98.

(43) Rothe, J.; Denecke, M. A.; Dardenne, K., Soft X-Ray Spectromicroscopy Investigation of the Interaction of Aquatic Humic Acid and Clay Colloids. *J. Colloid Interface Sci.* **2000,** *231*, (1), 91-97.

(44)Rowley, M. C.; Grand, S.; Verrecchia, É. P., Calcium-mediated stabilisation of soil organic carbon. *Biogeochemistry* **2017,** *137*, (1-2), 27-49.

(45) Song, F.; Li, T.; Wu, F.; Leung, K. M. Y.; Hur, J.; Zhou, L.; Bai, Y.; Zhao, X.; He, W.; Ruan, M., Temperature-Dependent Molecular Evolution of Biochar-Derived Dissolved Black

Carbon and Its Interaction Mechanism with Polyvinyl Chloride Microplastics. *Environ. Sci. Technol.* **2023,** *57*, (18), 7285-7297.

(46) Curti, L.; Moore, O. W.; Babakhani, P.; Xiao, K.-Q.; Woulds, C.; Bray, A. W.; Fisher, B. J.; Kazemian, M.; Kaulich, B.; Peacock, C. L., Carboxyl-richness controls organic carbon preservation during coprecipitation with iron (oxyhydr)oxide in the natural environment. *Commun. Earth Environ.* **2021,** *2*, (1), 229.

(47) Zhao, Y.; Moore, O. W.; Xiao, K.-Q.; Curti, L.; Fariña, A. O.; Banwart, S. A.; Peacock, C. L., The role and fate of organic carbon during aging of ferrihydrite. *Geochim. Cosmochim. Acta* **2022,** *335*, 339-355.

(48) Zhang, H.; Lu, Y.; Ouyang, Z.; Zhou, W.; Shen, X.; Gao, K.; Chen, S.; Yang, Y.; Hu, S.; Liu, C., Mechanistic insights into the detoxification of Cr(VI) and immobilization of Cr and C during the biotransformation of ferrihydrite-polygalacturonic acid-Cr coprecipitates. *J. Hazard. Mater.* **2023,** *448*, 130726.

(49) Zeng, Q.; Huang, L.; Ma, J.; Zhu, Z.; He, C.; Shi, Q.; Liu, W.; Wang, X.; Xia, Q.; Dong, H., Bio-reduction of ferrihydrite-montmorillonite-organic matter complexes: Effect of montmorillonite and fate of organic matter. *Geochim. Cosmochim. Acta***2020,** *276*, 327-344.

(50) Hu, S.; Zhang, H.; Yang, Y.; Wang, W.; Zhou, W.; Shen, X.; Liu, C., Reductive Sequestration of Cr(VI) and Immobilization of C during the Microbially Mediated Transformation of Ferrihydrite-Cr(VI)-Fulvic Acid Coprecipitates. *Environ. Sci. Technol.* **2023,** *57*, (22), 8323-8334.

(51) Grafe, M.; Eick, M. J.; Grossl, P. R.; Saunders, A. M., Adsorption of Arsenate and Arsenite on Ferrihydrite in the Presence and Absence of Dissolved Organic Carbon. *J. Environ. Qual.* **2002,** *31*, (4), 1115-1123.

(52) Sowers, T. D.; Stuckey, J. W.; Sparks, D. L., The synergistic effect of calcium on organic carbon sequestration to ferrihydrite. *Geochem. Trans.* **2018,** *19*, (1), 4.

(53) Sowers, T. D.; Adhikari, D.; Wang, J.; Yang, Y.; Sparks, D. L., Spatial Associations and Chemical Composition of Organic Carbon Sequestered in Fe, Ca, and Organic Carbon Ternary Systems. *Environ. Sci. Technol.* **2018,** *52*, (12), 6936-6944.

(54) Schwertmann, U.; Cornell, R. M., *Iron Oxides in the Laboratory: Preparation and Characterization, second completely revised and extended edition*. Wiley-VCH: Weinheim, Germany, 2000.

(55) Hansel, C.; Benner, S.; Neiss, J.; Dohnalkova, A.; Kukkadapu, R.; Fendorf, S., Secondary Mineralization Pathways Induced by Dissimilatory Iron Reduction of Ferrihydrite under Advective Flow. *Geochim. Cosmochim. Acta***2003,** *67*, 2977-2992.

(56) Benner, S. G.; Hansel, C. M.; Wielinga, B. W.; Barber, T. M.; Fendorf, S., Reductive Dissolution and Biomineralization of Iron Hydroxide under Dynamic Flow Conditions. *Environ. Sci. Technol.* **2002,** *36*, (8), 1705-1711.

(57) Hansel, C. M.; Benner, S. G.; Nico, P.; Fendorf, S., Structural constraints of ferric (hydr)oxides on dissimilatory iron reduction and the fate of Fe(II)3 3Associate editor: J. B. Fein. *Geochim. Cosmochim. Acta* **2004,** *68*, (15), 3217-3229.

(58) Bartlett, R.; James, B., Behavior of Chromium in Soils: III. Oxidation. **1979,** *8*, (1), 31-35.

(59) Borges, S. d. S.; Korn, M.; Costa Lima, J.; eacute; Luis Fontes, d., Chromium(III) Determination with 1,5-Diphenylcarbazide Based on the Oxidative Effect of Chlorine Radicals Generated from CCl4 Sonolysis in Aqueous Solution. *Anal. Sci.* **2002,** *18*, (12), 1361-1366.

(60) Kaiser, K.; Guggenberger, G., The role of DOM sorption to mineral surfaces in the preservation of organic matter in soils. *Org. Geochem.* **2000,** *31*, (7), 711-725.

(61) Namduri, H.; Nasrazadani, S., Quantitative analysis of iron oxides using Fourier transform infrared spectrophotometry. *Corros. Sci.* **2008,** *50*, (9), 2493-2497.

(62) Xiao, W.; Jones, A. M.; Collins, R. N.; Bligh, M. W.; Waite, T. D., Use of fourier transform infrared spectroscopy to examine the Fe(II)-Catalyzed transformation of ferrihydrite. *Talanta* **2017,** *175*, 30-37.

(63) Sheng, A.; Li, X.; Arai, Y.; Ding, Y.; Rosso, K. M.; Liu, J., Citrate Controls Fe(II)-Catalyzed Transformation of Ferrihydrite by Complexation of the Labile Fe(III) Intermediate. *Environ. Sci. Technol.* **2020**, 54 (21) 7309-7319.

(64) Bazilevskaya, E.; Archibald, D. D.; Martínez, C. E., Rate constants and mechanisms for the crystallization of Al nano-goethite under environmentally relevant conditions. *Geochim. Cosmochim. Acta* **2012,** *88*, 167-182.

(65) Boily, J.-F.; Szanyi, J.; Felmy, A. R., A combined FTIR and TPD study on the bulk and surface dehydroxylation and decarbonation of synthetic goethite. *Geochim. Cosmochim. Acta***2006,** *70*, (14), 3613-3624.

(66) Jones, A. M.; Collins, R. N.; Rose, J.; Waite, T. D., The effect of silica and natural organic matter on the Fe(II)-catalysed transformation and reactivity of Fe(III) minerals. *Geochim. Cosmochim. Acta***2009,** *73*, (15), 4409-4422.

(67) ThomasArrigo, L. K.; Mikutta, C.; Byrne, J.; Kappler, A.; Kretzschmar, R., Iron(II)-Catalyzed Iron Atom Exchange and Mineralogical Changes in Iron-rich Organic Freshwater Flocs: An Iron Isotope Tracer Study. *Environ. Sci. Technol.***2017,** *51*, (12), 6897-6907.

(68) Illés, E.; Tombácz, E., The effect of humic acid adsorption on pH-dependent surface charging and aggregation of magnetite nanoparticles. *J. Colloid Interface Sci.* **2006,** *295*, (1), 115-123.

(69) Amstaetter, K.; Borch, T.; Kappler, A., Influence of humic acid imposed changes of ferrihydrite aggregation on microbial Fe(III) reduction. *Geochim. Cosmochim. Acta* **2012,** *85*, 326-341.

(70) ThomasArrigo, L. K.; Byrne, J. M.; Kappler, A.; Kretzschmar, R., Impact of Organic Matter on Iron(II)-Catalyzed Mineral Transformations in Ferrihydrite-Organic Matter Coprecipitates. *Environ. Sci. Technol.* **2018,** *52*, (21), 12316-12326.

(71) Zhou, Z.; Latta, D. E.; Scherer, M. M., Natural organic matter inhibits Ni stabilization during Fe(II)-catalyzed ferrihydrite transformation. *Sci. Total Environ.* **2020,** *755*, 142612.

(72) Hansel, C. M.; Benner, S. G.; Fendorf, S., Competing Fe(II)-Induced Mineralization Pathways of Ferrihydrite. *Environ. Sci. Technol.* **2005,** *39*, (18), 7147-7153.

(73) Amonette, J. E.; Rai, D., Identification of Noncrystalline (Fe,Cr)(Oh)3 by Infrared Spectroscopy. *Clays Clay Miner.* **1990,** *38*, (2), 129-136.

(74) Lu, Y.; Hu, S.; Wang, Z.; Ding, Y.; Lu, G.; Lin, Z.; Dang, Z.; Shi, Z., Ferrihydrite transformation under the impact of humic acid and Pb: kinetics, nanoscale mechanisms, and implications for C and Pb dynamics. *Environ. Sci.: Nano* **2019,** *6*, (3), 747-762.

(75) Wu, Z.; Zhang, T.; Lanson, B.; Yin, H.; Cheng, D.; Liu, P.; He, F., Sulfidation of Ni-bearing goethites to pyrite: The effects of Ni and implications for its migration between iron phases. *Geochim. Cosmochim. Acta* **2023,** *353*, 158-170.

(76) Xia, X.; Liu, J.; Jin, L.; Wang, J.; Darma, A. I.; He, C.; Shakouri, M.; Hu, Y.; Yang, J., Organic Matter Counteracts the Enhancement of Cr(III) Extractability during the Fe(II)-Catalyzed Ferrihydrite Transformation: A Nanoscale- and Molecular-Level Investigation. *Environ. Sci. Technol.***2023**, 57 (36), 13496-13505.

(77) Sass, B. M.; Rai, D., Solubility of amorphous chromium(III)-iron(III) hydroxide solid solutions. *Inorg. Chem.* **1987,** *26*, (14), 2228-2232.

(78) Kaur, N.; Gräfe, M.; Singh, B.; Kennedy, B., Simultaneous Incorporation of Cr, Zn, Cd, and Pb in the Goethite Structure. *Clays Clay Miner.* **2009,** *57*, (2), 234-250.

(79) Jelavić, S.; Mitchell, A. C.; Sand, K. K., Fate of organic compounds during transformation of ferrihydrite in iron formations. *Geochem. Perspect. Lett.* **2020,** *15*, 25-29.

(80) Manceau, A.; Drits, V., Local structure of ferrihydrite and feroxyhite by EXAFS spectroscopy. *Clay Miner.* **1993,** *28*, (2), 165-184.

(81) Cudennec, Y.; Lecerf, A., The transformation of ferrihydrite into goethite or hematite, revisited. *J. Solid State Chem.* **2006,** *179*, (3), 716-722.

(82) Das, S.; Hendry, M. J.; Essilfie-Dughan, J., Transformation of Two-Line Ferrihydrite to Goethite and Hematite as a Function of pH and Temperature. *Environ. Sci. Technol.* **2011,** *45*, (1), 268-275.

(83) Schwertmann, U.; Stanjek, H.; Becher, H.-H., Long-term in vitro transformation of 2-line ferrihydrite to goethite/hematite at 4, 10, 15 and 25 C. *Clay Miner.* **2004,** *39*, (4), 433-438.

(84) Schwertmann, U.; Murad, E., Effect of pH on the Formation of Goethite and Hematite from Ferrihydrite. *Clays Clay Miner.* **1983,** *31*, (4), 277-284.

(85) Johnston, J. H.; Lewis, D. G., A detailed study of the transformation of ferrihydrite to hematite in an aqueous medium at 92°C. *Geochim. Cosmochim. Acta* **1983,** *47*, (11), 1823-1831.

(86) Zhao, Y.; Moore, O. W.; Xiao, K.-Q.; Curti, L.; Fariña, A. O.; Banwart, S. A.; Peacock, C. L., The role and fate of organic carbon during aging of ferrihydrite. *Geochim. Cosmochim. Acta* **2022**, *335*, 339-355.

(87) Hemingway, J. D.; Rothman, D. H.; Grant, K. E.; Rosengard, S. Z.; Eglinton, T. I.; Derry, L. A.; Galy, V. V., Mineral protection regulates long-term global preservation of natural organic carbon. *Nature* **2019,** *570*, (7760), 228-231.

(88) Xiao, K. Q., Zhao, Y., Liang, C., Zhao, M.Y., Moore, O.W., Otero-Farina, A., Zhu, Y.G., Johnson K., Peacock, C.L., Introducing the soil mineral carbon pump. *Nat. Rev. Earth Environ. 4*, (3).

(89) Kaiser, K.; Guggenberger, G., Sorptive stabilization of organic matter by microporous goethite: sorption into small pores vs. surface complexation. *Eur. J. Soil Sci.* **2007,** *58*, (1), 45-59.

(90) Xiao, K.-Q.; Moore, O.; Babakhani, P.; Curti, L.; Peacock, C., Mineralogical control on methylotrophic methanogenesis and implications for cryptic methane cycling in marine surface sediment. *Nat. Commun.* **2022**, *13*, (1), 2722.

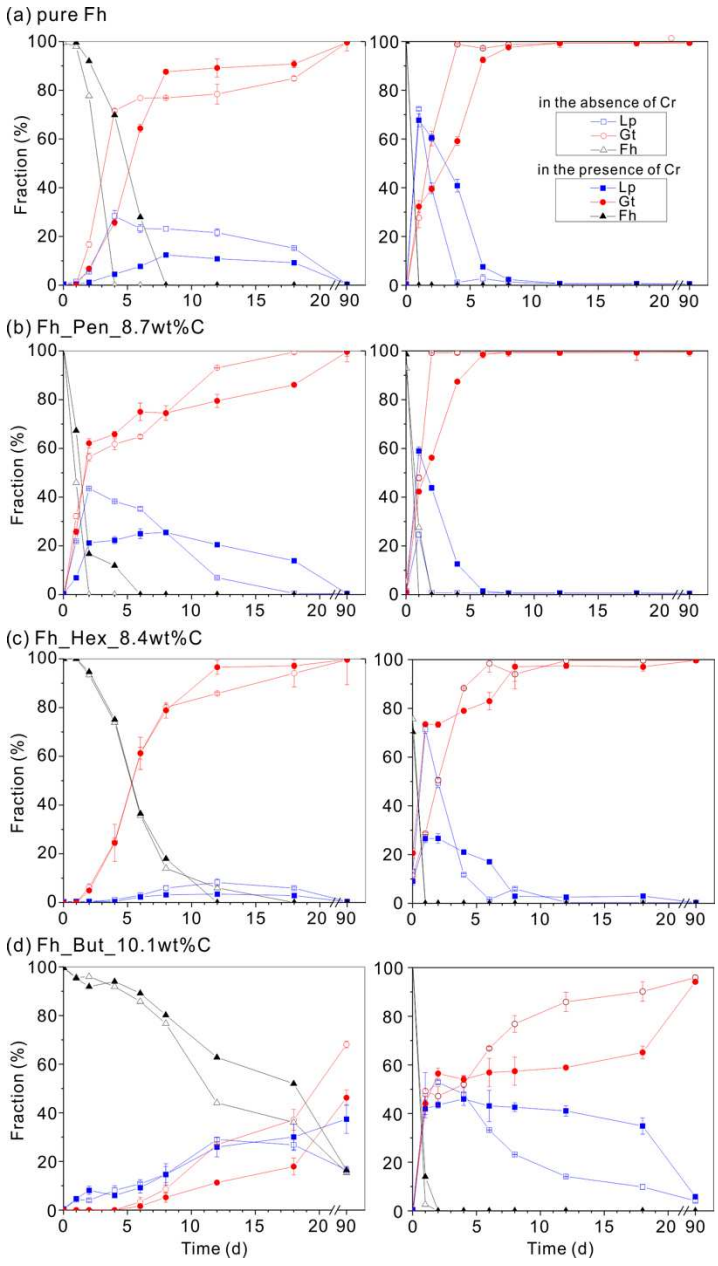

Figure 1. Relative proportions of Gt and Lp during the Fe(II)-catalysed transformation of pure Fh and Fh organominerals in the presence or absence of Cr at pH 5.75 and 7.00. Pen, Hex and But represent simple carboxyl-rich OC with one, two and three carboxyl groups, respectively.

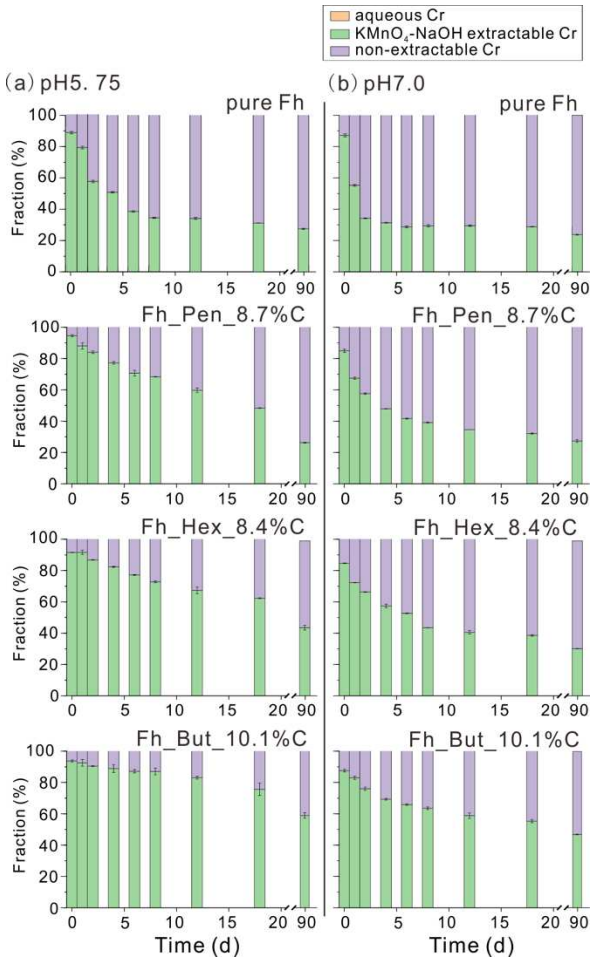

663

664 Figure 2. Temporal changes of Cr species during the Fe(II)-catalyzed transformation of pure Fh
665 and Fh organominerals at pH 5.75 and pH 7.00. Specifically, the first sampling was conducted
666 after adding Fe(II) for 0.5 h. Pen1/5, Hex2/6 and But3/7 represent simple carboxyl-rich OC with
667 one, two and three carboxyl groups, respectively.

668

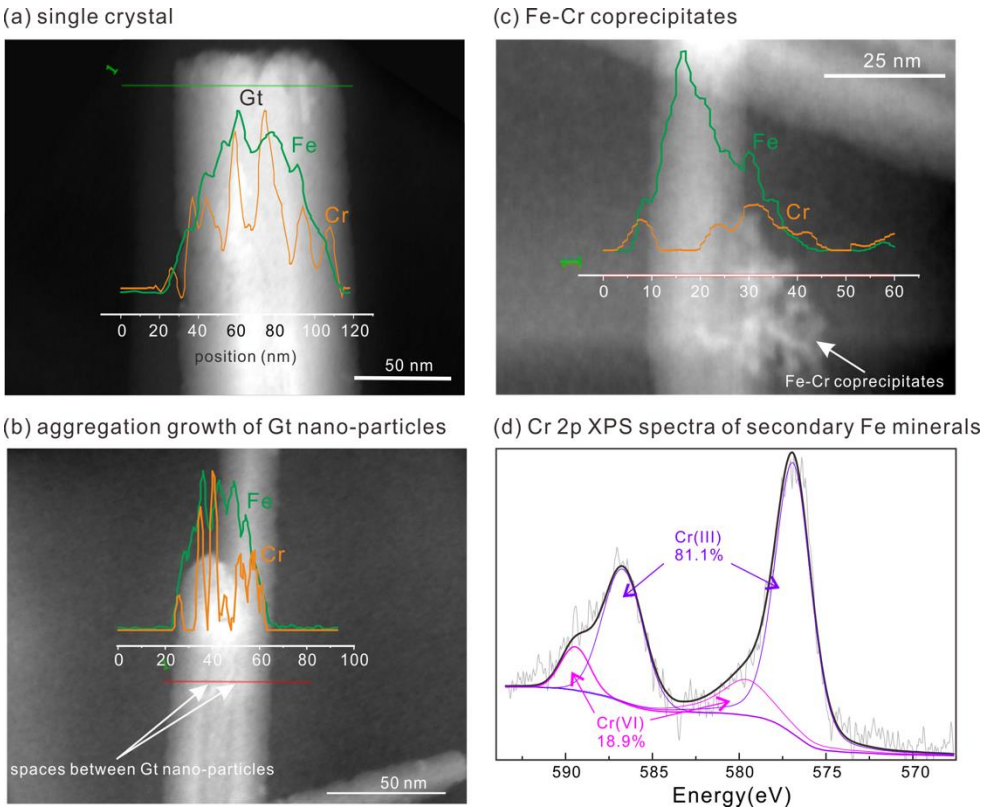

669

670 Figure 3. EDS line profiles and XPS spectra for secondary Fe minerals formed from pure Fh at pH
671 7.0 (a, b, c) and pH 5.75 (d) after 12-days reaction. a) Cr (orange line) and Fe (green line)
672 distribution of a single crystal of Gt; b) Cr and Fe distribution over the aggregation of Gt nano-
673 particles; c) Cr and Fe distribution of Fe-Cr coprecipitates; d) Cr(III/VI) species observed by Cr
674 2p XPS spectra.

675

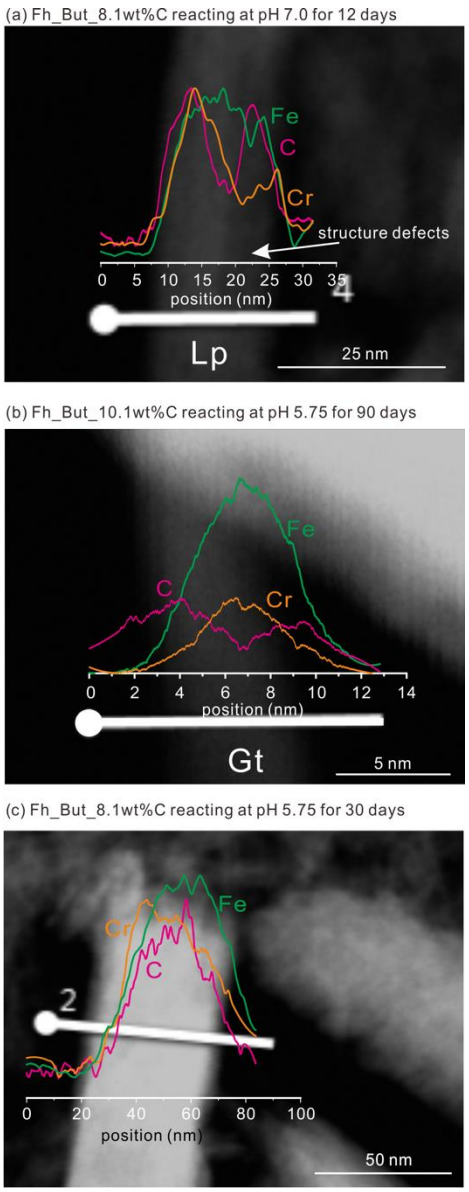

676

677 Figure 4. EDS line profiles of Fe (green), Cr (orange) and C (purple) distribution on representative
678 Fe minerals formed from Fe(II)-induced transformation of Fh_But 3/7 organominerals.

679

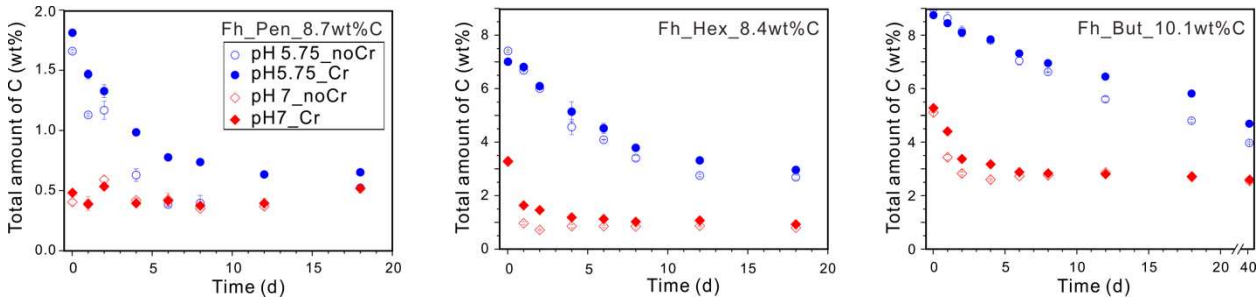

680

681

682 Figure 5. Temporal changes in the total amount of Ctotal-solid during Fe(II)-induced
683 transformation at pH 5.75 and pH 7.00 with and without Cr. Pen, Hex and But represent simple
684 carboxyl-rich OC with one, two and three carboxyl groups, respectively. Note differing scale on
685 y-axis for Fh_Pen_8.7wt%C.

686

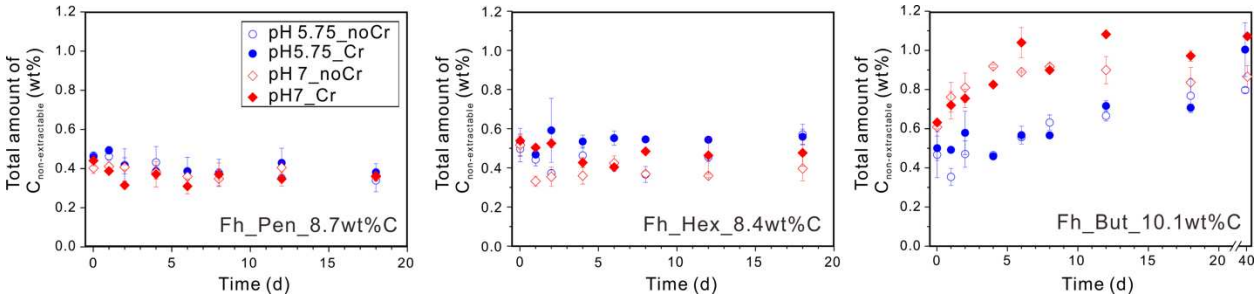

687

688 Figure 6. Temporal changes in the total amount of Cstrongly-bound in the Fh-organominerals solid
689 phase during Fe(II)-induced transformation at pH 5.75 and pH 7.00 with or without Cr. Cstrongly-
690 bound are operationally defined as OC are non-desorbable by 0.1 M NaOH. Pen1/5, Hex2/6 and
691 But3/7 represent simple carboxyl rich OC with one, two and three carboxyl groups, respectively.

692